



STUDY OF RESIDUAL STRESS AND MECHANICAL PROPERTIES OF 2Cr13 STAINLESS STEEL STEAM TURBINE BLADES BY DIFFERENT LASER SURFACE MODIFICATIONS

JIANHUA YAO¹, LIANG WANG¹, QUNLI ZHANG¹, ZHIJUN CHEN¹ and V.S. KOVALENKO²

¹Zhejiang University of Technology, Zhejiang, China

²Laser Technology Research Institute of the NTUU «Kiev Polytechnic Institute», Kiev, Ukraine

As the key part of steam turbine, the blades work under the impact of high-speed steam and water droplet. Water droplet erosion on the inlet edge area is considered as the common failure pattern. In this paper, three laser surface modification ways including quenching, remelting and alloying were used to avoid water droplet erosion on the 2Cr13 stainless steel turbine blades. Residual stress and mechanical properties of the three modification methods were compared respectively. The result shows that the surface microhardness of blades increases after laser surface modifications. The tensile strength of the material is improved and meanwhile both the elongation percentage and reduction in cross sectional area are decreased. The impact fractures were all brittle fractures. The laser hardening zone presents residual compressive stress, and the heat-affected zone presents small transverse tensile stress.

Keywords: laser surface modification, turbine blade, residual stress, mechanical properties

Steam turbine blades are critical components in power plants, which convert the linear motion of high temperature and high pressure steam flowing down a pressure gradient into rotary motion of the turbine shaft [1, 2]. Water droplet erosion is a well-known phenomenon on the moving blades operating at the low-pressure end of steam turbines. It is initiated by «small», primary droplet condensate in bulk of the supercooled steam in the flow, and then gets separated on the blade surface and generates secondary «large» droplets, which causes erosion [3].

To improve the water droplet erosion resistance of low-pressure blades, laser cladding of stellite alloy has been applied, which resulted in generation of residual stresses in the cladding region [4]. The reason is that the difference in thermal expansion between the stellite alloy and parent metal during cooling, thermal strain caused by the differences in heating/cooling at differing locations and the directional stiffness within the sections present [5].

In order to overcome the above disadvantage of high residual stress after laser cladding and to obtain dense bonding hardening layer, laser quenching, laser remelting and laser alloying techniques were introduced to strengthen steam turbine blades and to maintain high surface hardness as well [6, 7]. As a kind of hardenable, chromium stainless steels 2Cr13 combines the superior wear resistance of high carbon alloy with the excellent corrosion resistance of chromium stainless steel. Adding sufficient amounts of carbon to chromium stainless steel, the microstructure of the alloy has the capability to transform into something

featured excellent strength, hardness, edge retention, and wear resistance through proper heat treatment (hardening) process. The presence of sufficient chromium will impart the necessary corrosion resistance and form chromium carbide particles to enhance the wear resistance of the given alloy. Due to the virtues mentioned above, 2Cr13 is applied in the area of dental, surgical instruments and nozzles, as well as steam turbine blades.

In this article, the techniques of laser quenching, laser remelting and laser alloying were applied on the 2Cr13 steam turbine blades because of their high surface hardness and low residual stress. Laser quenching is a technology which using the laser heating and self-cooling to complete the quenching processing. Laser remelting is a material surface rapid melting and solidifying processing. By adding alloying material to the substrate surface, laser alloying technique could acquire outstanding surface quality while maintaining the bulk material properties. The three techniques should be applied in different type of blades under different operating environments, substituting for the traditional hardening techniques on blades. Then the blades service life will be extended and the units high efficiency operating will be maintained. The microstructure, microhardness, mechanical properties and residual stress of strengthened layer by different techniques were researched and discussed.

Experimental procedure. The substrate material is 2Cr13 which has been processed by hardening and tempering (heating to 980–1035 °C, followed by quenching in oil, then tempering at 220–300 °C). The chemical composition of the 2Cr13 stainless steel is as follows, wt. %: 0.16–0.21 C; 12 Cr; <1 Si; <0.8 Mn; <0.03 S; <0.04 P; balance — Fe.

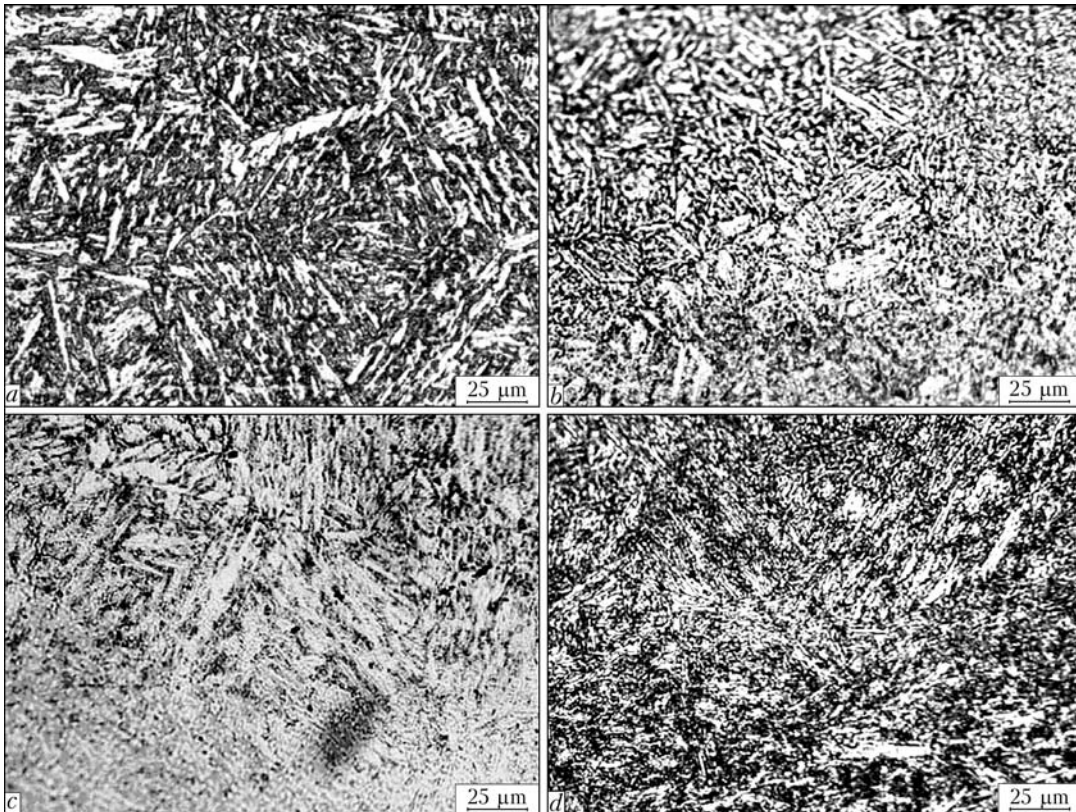


Figure 1. Microstructure of the middle part of laser hardening layer: *a* – substrate; *b* – laser quenching (sample 1); *c* – laser remelting (sample 2); *d* – laser alloying (sample 3)

Figure 1, *a* shows the microstructure of 2Cr13 stainless steel with tempered sorbite. The surface was cleaned by sonication in acetone or alcohol. When the surface of the sample was clean and dry, the alloying powder mixed with some binder was smeared on the surface. The experiments were carried out by a 7 kW rated power CW CO₂ laser system with a CNC controlled working table. Three different optimized laser processing parameters were used to strengthen the 2Cr13 steam turbine blades (Table 1). Samples 1, 2 and 3 were processed by laser quenching, remelting and alloying respectively. The chemical composition of laser surface alloying material for the three samples was as follows, wt. %: 1.3 Si; 2.86 Cr; 3.29 Ni; 0.98 Fe; 40.24 W; 51.33 Co.

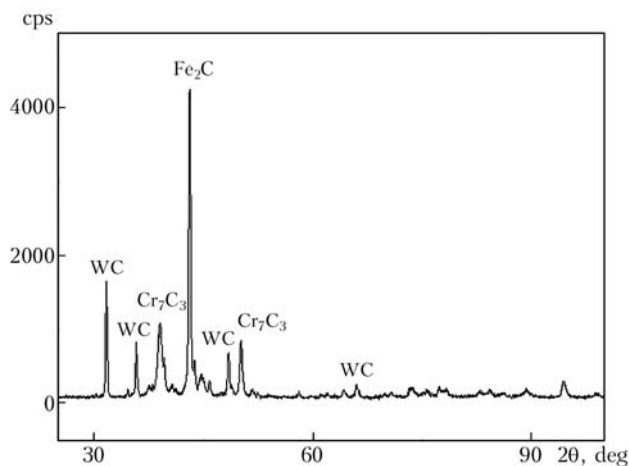


Figure 2. XRD pattern of the top of alloyed layer surface

The mechanical properties were tested by WE-30 hydraulic universal test machine. The microstructure and composition were observed using the FEI-SIRION100 scanning electronic microscope (SEM) equipped with Thermo NORAN energy diffraction spectrometer (EDS). The XRD patterns of the alloyed surface were measured on Thermo SCINTAG X" TRA. The microhardness was tested by the HDX100 microhardness tester with the load of 200 g and the action time of 15 s. The residual stress was tested by X-350A residual stress tester.

Results and discussion. *Microstructure and microhardness.* After laser quenching (sample 1), the fine martensites with staggered distributing are found in strengthened layer (Figure 1, *b*). During the rapid heating and rapid cooling process of laser hardening, the growth of austenite is restrained, and the high degree refined microstructure forms, which results in the increase of the surface hardness. After laser remelting (sample 2), the surface of the remelting layer appears to be as-cast structure, and the martensite in

Table 1. Optimized laser parameters at laser beam size of 2 × 8 mm²

| Sample No. | Power, kW | Scanning speed, mm/min | Added alloying material |
|------------|-----------|------------------------|-------------------------|
| 1 | 1.2 | 300 | No |
| 2 | 1.6 | 500 | Same |
| 3 | 1.6 | 500 | Yes |



HV0.2

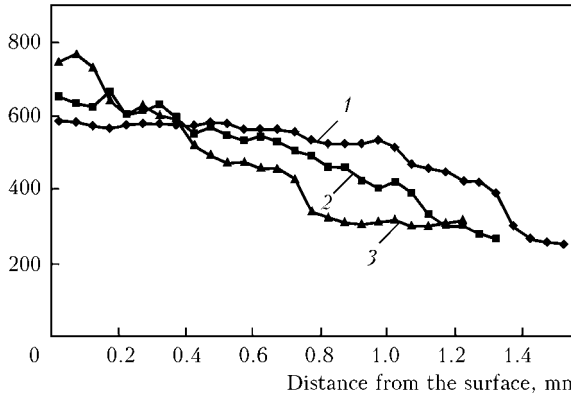


Figure 3. Cross-section hardness after laser hardening of samples 1-3 (1-3)

HAZ is bigger than in substrate (Figure 1, c). Compared with laser remelting, the microstructure after laser alloying is much finer (Figure 1, d). During the laser alloying process, under the high laser power irradiating, the surface of the sample is molten and the alloying materials are fusing into the melting layer simultaneity, which can be proved by the EDS results (wt. %: 0.29 Si; 13.78 Cr; 10.59 W; 0.47 Ni; 0.46 V; 1.32 Mo; Fe and C – balance). According to XRD results (Figure 2) the phases of the alloyed layer include WC, Fe₂C and Cr₇C₃. The highly decentralized WC hard phases will be the main reason for the microhardness improvement (Figure 3). The hardenability of the materials is enhanced because of the existence of chromium. Meanwhile, the hardness is increased due to the formed Cr₇C₃ hard phases. As an element to expand the austenite region, the added nickel prevents the formation of the second-phase particles and improves the surface erosion resistance performance.

Table 2. Tensile test results after laser processing

| Sample No. | Tensile strength, MPa | Elongation, % | Reduction in area, % |
|------------|-----------------------|---------------|----------------------|
| 1 | 881.51 | 15.93 | 39.40 |
| 2 | 860.14 | 13.88 | 33.43 |
| 3 | 863.88 | 13.47 | 32.77 |
| Substrate | 850.65 | 15.97 | 41.50 |

Table 3. Impact test results after laser processing

| Sample No. | Impact energy, J | Toughness, J/cm ² |
|------------|------------------|------------------------------|
| 1 | 37.3 | 46.67 |
| 2 | 37.4 | 46.83 |
| 3 | 37.0 | 46.25 |
| Substrate | 37.7 | 47.08 |

The cross-section hardness after laser hardening was tested from surface to substrate (see Figure 3). Indicated from this Figure, the thickness of laser quenching layer (sample 1) is about 1.2 mm, the thickness of laser remelting layer (sample 2) is about 0.9 mm, and the thickness of laser alloying layer (sample 3) is about 0.4 mm. The hardness is declined from the surface to substrate with gradient. The hardening layer hardness of sample 1 is lower than that of both sample 2 and sample 3. However, the depth of quenching layer is greater than in sample 2 and sample 3. The lower speed results in thicker heating depth and the finer martensites with staggered distribution are transformed, which is the primary hardening mechanism of laser quenching (see Figure 2). Because of higher laser scanning speed and rapid cooling speed,

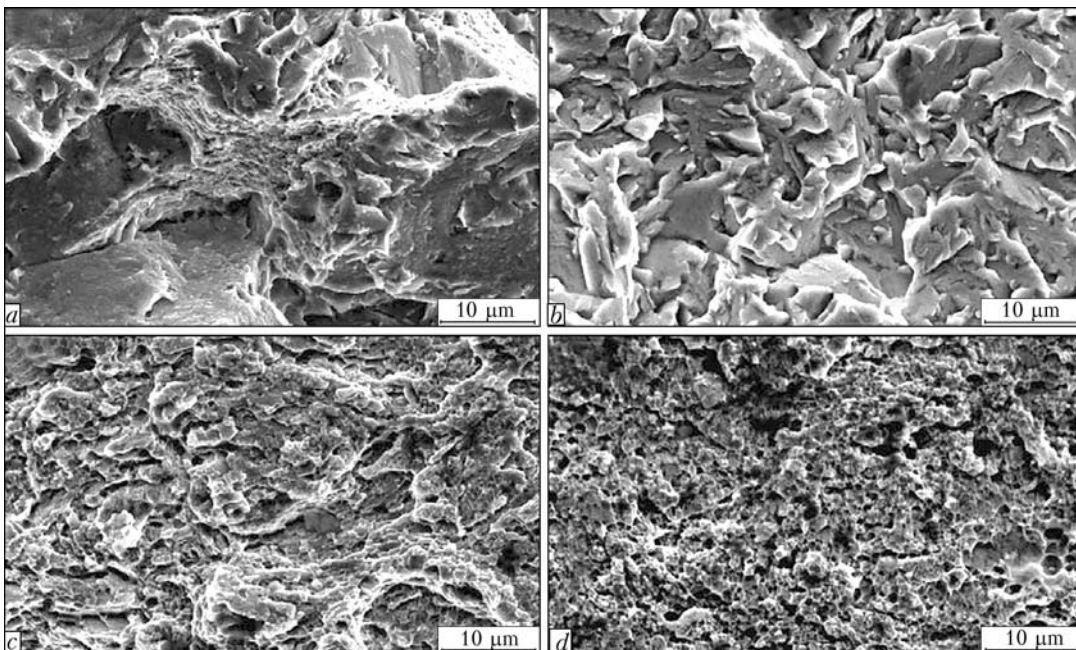


Figure 4. Impact fracture pattern after laser hardening: a – substrate; b – laser quenching (sample 1); c – laser remelting (sample 2); d – laser alloying (sample 3)



the hardening layer of sample 2 and 3 is thinner than in sample 1. The largest hardness value is found in sample 3 due to the added alloying material and hardness phases (WC , Fe_2C and Cr_7C_3) after laser processing.

Mechanical properties. The tensile test results after laser processing are shown in Table 2. After laser processing, the tensile strength of the samples are improved, but the elongation and the reduction in cross-sectional area are reduced. After laser quenching (sample 1), the grains are refined, so that the tensile strength improves a little. Compared with the laser quenching technology, laser remelting and alloying need higher laser power density to melt the surface. Because of the as-cast microstructure, the microscopic mechanical properties decline, resulting in the reduction of elongation.

The impact results after laser processing are shown in Table 3. After laser processing, the impact toughness of the samples are all reduced because of the residual stress and brittle martensite after laser radiating.

Figure 4 shows the impact fracture pattern of the substrate and the three samples. The plentiful cleavage planes are found in substrate, but there are partial dimples. After laser quenching (sample 1), the cleavage planes are a bit smaller. The pattern of samples 2 and 3 (after laser remelting and laser alloying) are also cleavage planes. Because of the higher laser power and higher cooling speed, the grains are much finer than those of sample 1, so the cleavage planes are smaller than those of the substrate and sample 1.

Residual stress. Figure 5 shows the sketch map of laser hardening section. The laser hardening section is the convex surface of blades, which section would be suffered a number of water droplets impact in the last-stage of steam turbines. To avoid the integral distortion and reduce the cost, only local section was chosen to strengthen. Residual stress test points of the laser hardening section are also shown in Figure 5. Points 1, 3–8 are in the laser hardening section, points

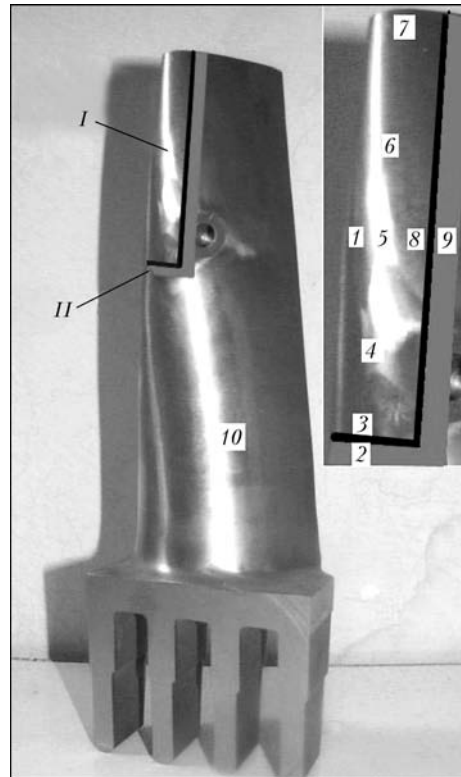


Figure 5. Sketch map of residual stress test points distribution in laser hardening section: I – laser strengthening section; II – HAZ

2 and 9 – in the HAZ and point 10 – in the substrate for comparison.

The residual stress distributions of the blades after laser quenching and laser alloying are shown in Figure 6, a, b. The processing parameters of laser remelting is the same with laser alloying, so that the residual stress test result of laser remelting is approximately considered as the same with the laser alloying. The transverse stress and longitudinal stress of original blade surface (see point 10 in Figure 5) are -231 and -212 MPa respectively. The transverse residual stress in HAZ presents tensile stress, and the longitudinal residual compressive stress in HAZ is much lower than in laser processing section (points 2 and 9). The re-

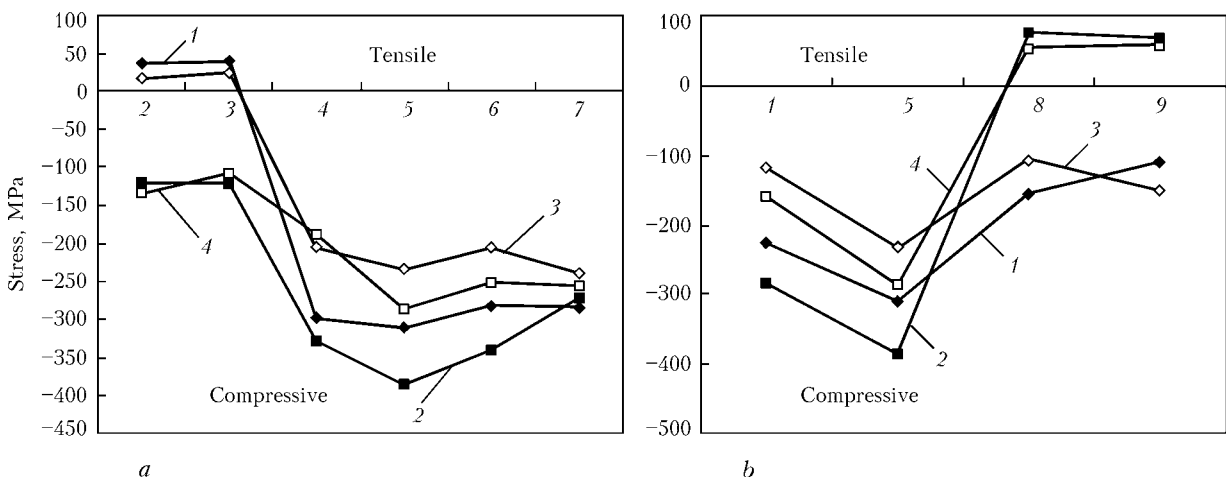


Figure 6. Residual stress distributions of the blades after laser quenching (points 2–7) (a) and laser alloying (points 1, 5, 8, 9) in transverse (1, 3) and longitudinal (2, 4) directions



sidual stress state of points 2 and 3 are similar to the points 8 and 9. These points are all beside the laser scanning initial position with lower laser energy, so the effect of relief annealing under laser lower irradiating energy results in different residual stress state from the section under laser high irradiating energy. The residual stresses in high energy section of laser processing are all present compressive stress. It is obvious that the residual compressive stress after laser alloying is larger than that of laser quenching, whether the transverse direction or longitudinal direction. On the effect of laser fast heating and rapid cooling, the material occurs phase-change, transforming into the martensite during laser quenching processing, which results in the volume expanding. Therefore the material surface presents residual compressive stress. The laser alloying needs higher laser power, so the blade surface processing section is melted. Under the short processing of rapid cooling after laser heating, the molten material is solidified instantly and the original stress state is changed simultaneously [8]. In the practical applications, the appropriate compressive stress is favorable, while the tensile stress will reduce the fatigue life of the blades.

CONCLUSIONS

1. The thickest hardening layer is found after laser quenching, but its hardness is lower than in laser remelting and laser alloying. The martensites with staggered distributing are the main microstructure of strengthened layer after laser quenching. The microstructure in laser remelting is finer than in laser quenching. The laser alloying has the highest hardness ($HV0.2-780$) but thin harden layer. The WC, Fe_2C and Cr_7C_3 are the main hardening phases in the alloyed layer.

2. After three laser techniques processing, the tensile strength of the material is improved and meanwhile both the elongation percentage and reduction in cross sectional area are decreased. The impact resistance of material is not declined after laser hardening. From the impact fracture SEM analysis, the impact fractures of

hardening layers are plentiful brittle fractures. With the increasing of laser scanning speed and laser power, the grains of cleavage planes are getting smaller gradually. The smallest grain of cleavage plane is present to the sample of laser alloying.

3. After laser processing, the laser hardening zone presents high residual compressive stress in both directions. But the edge of laser scanning zone and HAZ presents transverse tensile stress and lower longitudinal compressive stress. Compared with the surface residual stress after laser quenching, the residual compressive stress of laser alloying is increased more than 35 %.

The contrast and discussion of the three different laser hardening techniques on steam turbine blades will be the favorable reference to choose proper laser processing technique to harden turbine blades surface.

Acknowledgements. *The authors would like to appreciate financial support from International Cooperation Project of Ministry of Science and Technology (JG-JD-2008001) and the Open Foundation of Provincial Key Discipline of Advanced Manufacturing Technology (AMT200506-009).*

1. Wei-Ze, W., Fu-Zhen, X., Kui-Long, Z. et al. (2006) Failure analysis of the final stage blade in steam turbine. *Mater. Sci. Eng. A*, **437**, 70-74.
2. Mazur, Z., Garcia-Illescas, R., Aguirre-Romano, J. (2008) Steam turbine blade failure analysis. *Eng. Fail. Anal.*, **15**, 129-141.
3. Mann, B.S., Arya, V. (2003) HVOF coating and surface treatment for enhancing droplet erosion resistance of steam turbine blades. *Wear*, **254**, 652-667.
4. Kathuria, Y.P. (2000) Some aspects of laser surface cladding in the turbine industry. *Surf. Coat. Technol.*, **132**, 262-269.
5. Bendeich, P., Alamb, N., Brandt, M. et al. (2006) Residual stress measurements in laser clad repaired low pressure turbine blades for the power industry. *Mater. Sci. Eng. A*, **437**, 70-74.
6. de Camargo, J.A.M., Cornelis, H.J., Cioffi, V.M.O. et al. (2007) Coating residual stress effects on fatigue performance of 7050-T7451 aluminum alloy. *Surf. Coat. Technol.*, **201**, 9448-9455.
7. Borrego, L.P., Pires, J.T.B., Costa, J.M. et al. (2007) Fatigue behaviour of laser repairing welded joints. *Eng. Fail. Anal.*, **14**, 1586-1593.
8. Frenka, A., Marsdena, C.F., Wagnier, J.-D. et al. (1991) Influence of an intermediate layer on the residual stress field in a laser clad. *Surf. Coat. Technol.*, **45**, 435-441.